Supplemental Figure 1

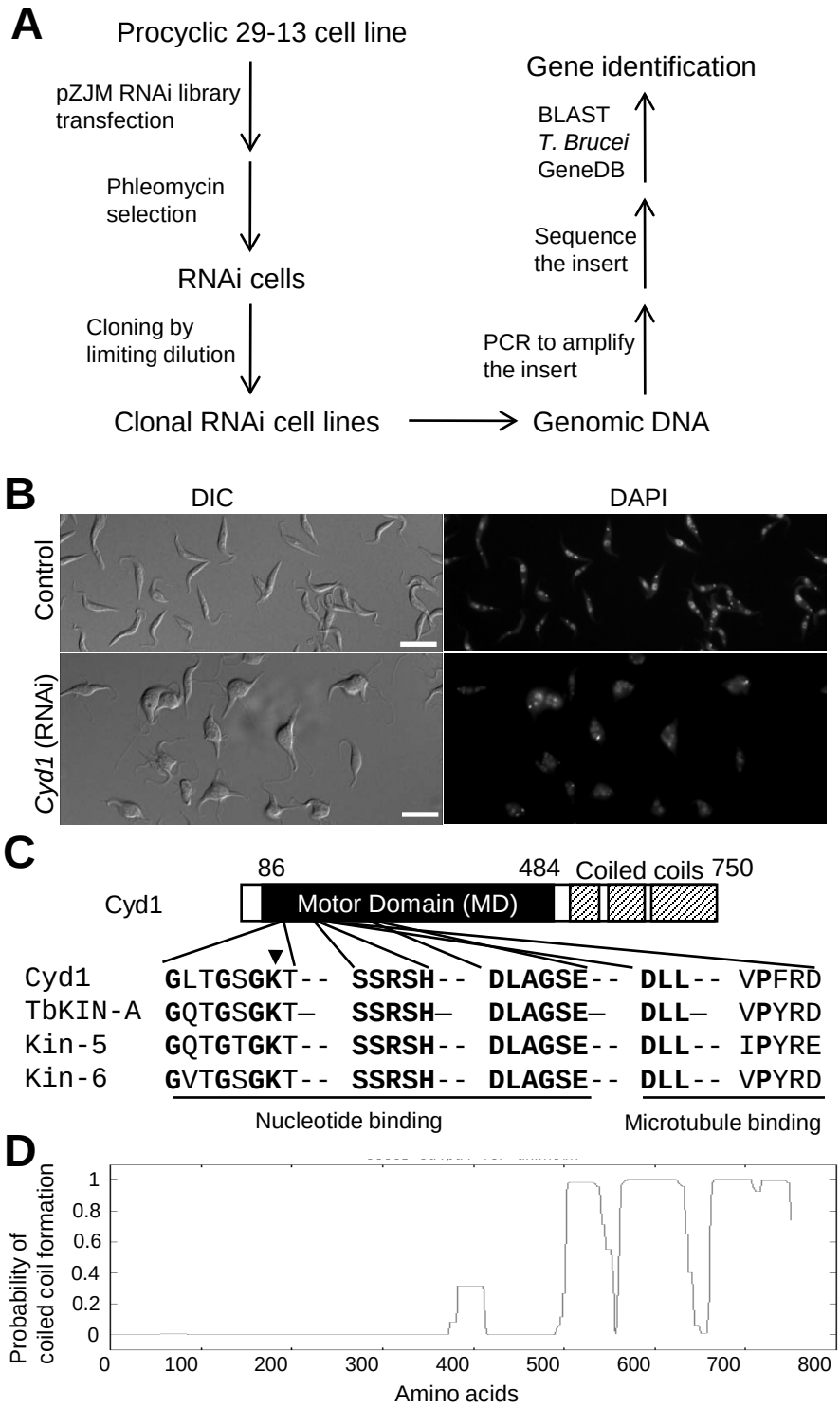

Supplemental Figure 1. Identification of *TbKIN-C* gene. (A). Strategy for identification of cytokinesis defect genes by genomic RNAi screen in the procyclic form of *T. brucei*. (**B**). Phenotypes of the TbKIN-C mutant identified by RNAi screen. Bars: 10 µm. (**C**). Schematic representation of the structure of TbKIN-C. Alignment of the conserved motifs in the motor domain of TbKIN-C with that of trypanosome TbKIN-A, and human Kin-5 and Kin-6 kinesins is presented. Black arrowhead pointed to the conserved lysine residue that is essential for ATP binding and is mutated to alanine in TbKIN-C (K196A) for *in vitro* ATPase assays. (**D**). Location of the coiled-coil motifs at the C-terminus of TbKIN-C as predicted by the COILs program.

Supplemental Figure 2

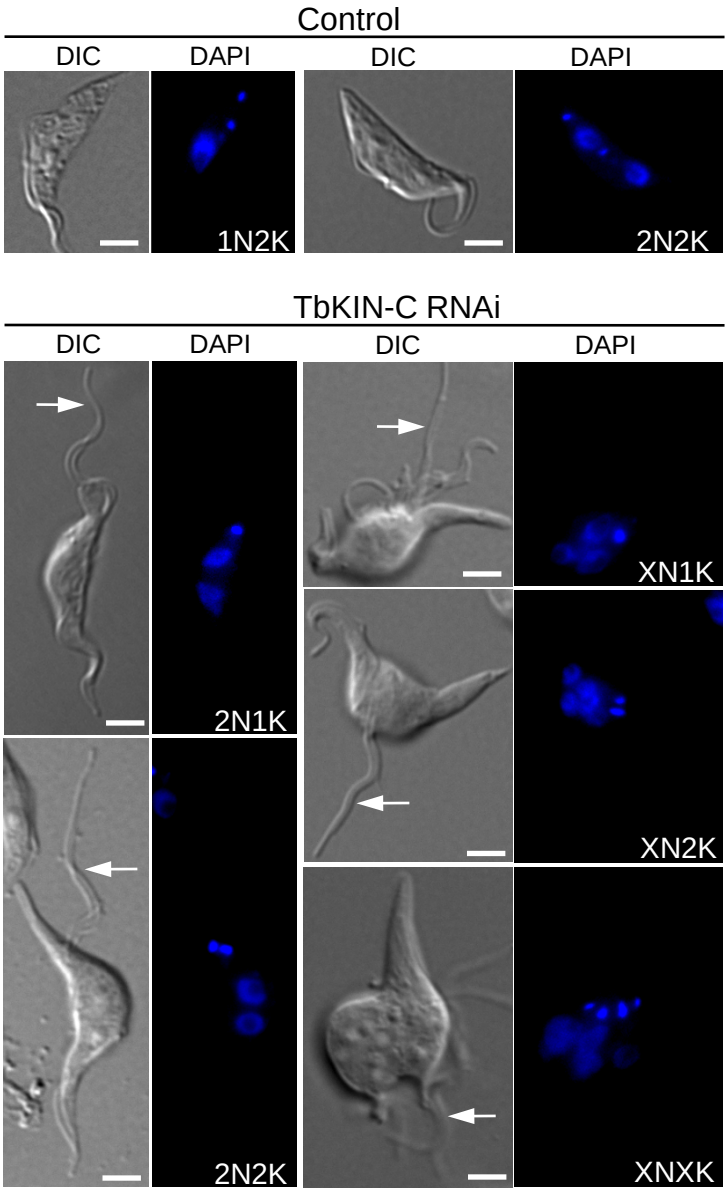

Supplemental Figure 2. Morphology of TbKIN-C RNAi cells. Cells were fixed with paraformaldehyde and stained with DAPI for nuclear and kinetoplast DNA. The arrows pointed to detached flagellum. Bars: 2 µm.

Supplemental Figure 3

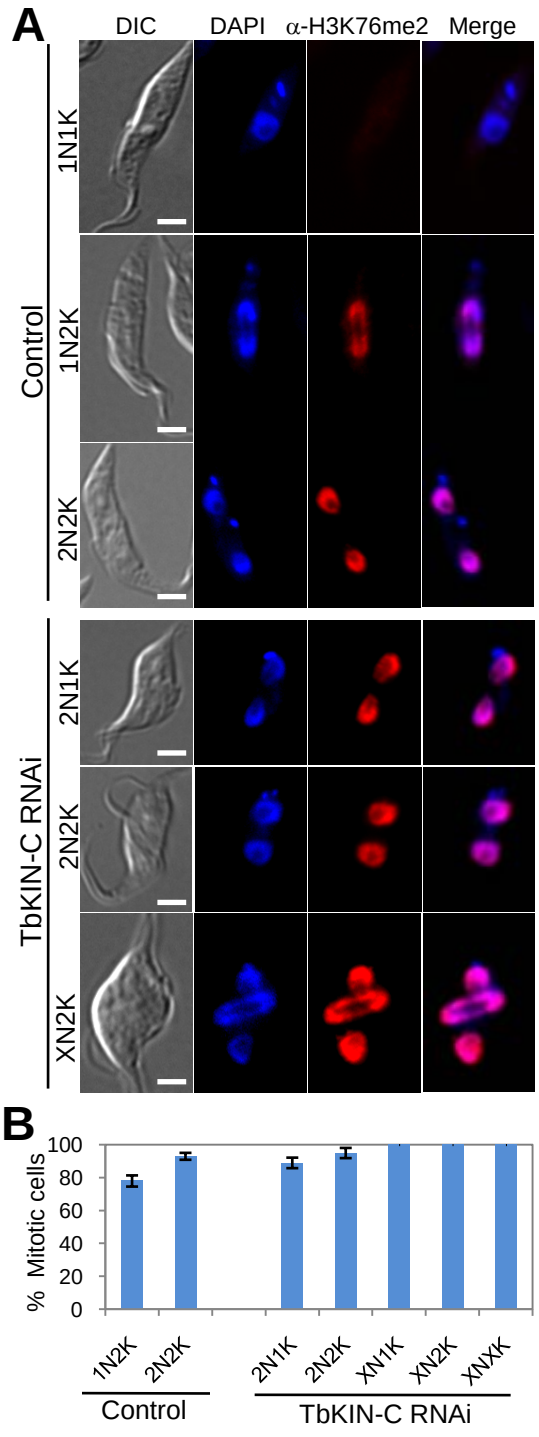

Supplemental Figure 3. RNAi of TbKIN-C does not inhibit mitotic progression in the procyclic form of *T. brucei*. (**A**). Effect of TbKIN-C RNAi on mitotic progression in the procyclic form of *T. brucei*. Control and TbKIN-C RNAi cells were fixed and stained with anti-H3K76me2 antibody, a mitotic marker in trypanosomes. Bars: 2 µm. (**B**). Percentage of mitotic cells in control and TbKIN-C RNAi cells as determined by anti-H3K76me2 antibody staining. Data are presented as the mean percent ±S.D. of ~200 cells counted from three independent experiments.